A Temperature and Emissivity Separation Technique for Thermal Hyperspectral Imagers

Dr. Pierre Lahaie
Data Exploitation Group
Optronic Surveillance Section, DRDC Valcartier
2459 Pie-XI Blvd. North
Val-Bélair, Québec

pierre.lahaie@drdc-rddc.gc.ca

ABSTRACT

The construction of very good hyperspectral sensors operating in the thermal infrared bands from 8 to 12 microns arouses much interest for the development of data exploitation tools. Temperature emissivity separation (TES) algorithms are very important components of a future toolbox, because they make it possible to extract these two fundamental targets' parameters. The emissivity relies on the nature of the target's surface materials, while the temperature gives information related to their use and relationship with the environment. The TES technique presented in this paper is based on iteration on temperature principle, where a total square error criterion is used to estimate the temperature. The complete procedure is described in the paper. Its sensitivity to noise is studied and a mathematical behavior model is provided. The model is validated through a Monte-Carlo simulation of the technique's operation.

1.0 INTRODUCTION

In the long wavelength infrared (LWIR) band, extending from 8 to 12 microns, the temperature and the emissivity can be defined as the fundamental parameters of the imaged material or targets. The emissivity provides information related to the target's nature while the temperature relates to its relationship with the environment or to its activity. Another very interesting feature of the LWIR bands is that the imagery could be acquired by day or night.

The processing chain surrounding calibrated thermal infrared hyperspectral imagery leading to the extraction of the imaged material fundamental properties are atmospheric compensation followed by temperature-emissivity separation. The atmospheric compensation is the process by which the atmospheric transmittance and path radiance are removed from the imagery. This step provides two important results: the ground-leaving radiance and the atmospheric downwelling irradiance. The path radiance is the energy generated by the atmosphere on the path from the target to the sensor. The transmittance is the amount of energy emitted by the ground and lost on the path from the target to the sensor. The downwelling irradiance is the energy incident on the target originating from the hemisphere above the target; it is often converted to radiance by assuming lambertian reflection from the target. Finally, the ground-leaving radiance is the energy leaving the target and is the combination of the target's self radiation and reflection of the atmospheric downwelling irradiance.

Lahaie, P. (2005) A Temperature and Emissivity Separation Technique for Thermal Hyperspectral Imagers. In *Emerging EO Phenomenology* (pp. 4-1 – 4-14). Meeting Proceedings RTO-MP-SET-094, Paper 4. Neuilly-sur-Seine, France: RTO. Available from: http://www.rto.nato.int/abstracts.asp.

Using the downwelling irradiance and the ground-leaving radiance, it is possible to extract the emissivity and the temperature of a target. The downwelling irradiance acts in the process as the reference. This principle has been used by Borel [1] and resulted in the ISSTES algorithm. This algorithm has subsequently been studied thoroughly by Ingram and Muse [2]. In our technique, we use the downwelling irradiance as the reference for the emissivity. We also use iteration for the determination of temperature, like what is done in Borel's procedure. Our technique's difference from ISSTES lies in the method used for selecting the right temperature and its corresponding emissivity. That difference leads to an increase in resistance to noise and to impairments such as the wrong estimation of the downwelling irradiance.

The paper is arranged as follows. In section 2 the assumed signal is described. Section 3 describes the general algorithm and highlights its most important features. Section 4 is devoted to a sensitivity analysis for noise and section 5 provides some experimental results obtained from ground sensing. Finally, the conclusion is presented in section 6.

2.0 SIGNAL MODEL

A complete signal model, taking into account every features of the atmosphere, is very complicated. It involves phenomenon such as heat-generated signal by ground objects and the atmosphere, scattering by the atmosphere (aerosols and clouds), absorption by the surface and by the atmosphere. If every single phenomenon was taken into account perfectly, a forward computation could be possible, but the inversion rapidly end into an intractable problem. One solution to that problem is to specify conditions for which the model possesses a simpler solution. A more tractable, but still very complicated situation arises when a clear sky is the weather condition. For a given spectral band, the signal model becomes:

$$L_{mn} = \int_0^{\infty} f_n(\sigma)\left[\left(\varepsilon(\sigma)B_T(\sigma) + \frac{(1-\varepsilon(\sigma))}{\pi}\int_0^{\pi/2}\int_0^{2\pi} L_i(\sigma,\theta,\phi)\sin(\theta)\cos(\theta)\,d\theta\,d\phi\right)\tau(\sigma) + L_p(\sigma)\right]d\sigma \qquad (1)$$

where σ is the wavenumber scale. This scale will be used throughout this paper since we also use it in conjunction with MODTRAN and with the instruments used to acquire data (ABB-Bomem Michelson interferometer). The term L_{mn} is the measured radiance in band n and f_n is a normalized weighting function for the spectral response of the instrument. ε is the emissivity of the target, B_T is the Planck function at temperature T. L_i is the atmospheric radiance incident on the surface from the sky from direction (θ, ϕ), τ is the atmospheric transmittance on the path from the target to the sensor and L_p is the path radiance accumulated from the target to the sensor and is given by:

$$L_p = \int_0^{a} B(T(y),\sigma)\left(-\frac{d\tau}{dy}\right)\exp\left(-\int_y^{a}\alpha(y',\sigma)\,dy'\right)dy \qquad (2)$$

where $T(y)$ is the temperature of the atmosphere at elevation y and α is the extinction coefficient of the atmosphere at elevation y. In this model the influence of single scattering by aerosol particles is neglected as a contribution to the signal. The aerosols' effects are considered however, in the extinction coefficient. Another simplification takes place in the reflective characteristics of the targets that are considered to be lambertian. Directional reflection peculiarities of targets are discarded in the model. The mathematical simulation of a potential sensor measurement therefore requires: the knowledge of the sensor's characteristics such as the spectral response of each of its bands; the target's characteristics, which are the spectral emissivity, reflection characteristics and its temperature; and the complete knowledge of the atmosphere, which are the temperature, the pressure and the humidity gradients.

The clear sky model needs to be simplified even more with the use of some physical assumption. The targets' emissivities can be assumed constant within the bounds of each band. This holds also for the blackbody function. This means that a bulk transmittance can be used for the whole band. The downwelling irradiance is spectrally highly variable. The bulk transmittance for the computation of its reflection transmission through the atmosphere cannot be used if high precision is required. However, if the sky is clear and the atmosphere equivalent temperature is much smaller than the ground temperature, in conjunction with generally high target emissivity renders marginal the contribution of downwelling irradiance. The bulk transmittance can therefore be used as an approximation for the reflected downwelling irradiance contribution. This will introduce more difficulties for processing of highly reflective targets, but since these targets are already extremely difficult to process, it does not increase the burden too heavily. The path radiance is additive and can therefore be considered separately. For any given band, the model can be simplified to provide the following equation:

$$L_{mn} = \left(\varepsilon_n B_n(T) + (1-\varepsilon_n)\frac{L_s}{\pi} \right)\tau_n + L_{pn} + N \tag{3}$$

In the remainder of the document, the π factor dividing the L_s contribution of atmospheric downwelling irradiance will be omitted. It must however be kept in mind that the L_s variable is been converted into radiance through this transformation. The bracketed part of the preceding equation is known as the ground-leaving radiance. The N variable is the sensor added noise for the band of interest. The removal of the path radiance and of the transmittance constitutes the first component of the processing chain i.e. the atmospheric compensation. This provides the ground-leaving radiance. This last quantity can be measured directly by a ground spectrometer and this way data can be gathered to verify specifically a temperature-emissivity separation algorithm. The signal model used in the remainder of the paper is therefore:

$$L_{mn} = \varepsilon_n B_n(T) + (1-\varepsilon_n)L_{sn} + \frac{N}{\tau_n} \tag{4}$$

3.0 ALGORITHM DESCRIPTION

3.1 Introduction

The TES system is built around the minimization of an error function. The error function can be the total square error or the total absolute error. In the total square error case, an error is computed for each band and the squares of band results are added together. For the total absolute error, the absolute values of the error in each band are added together. The system is assumed linear in the region of the minimum error and for this reason the two error computation methods should be unbiased and therefore generate similar minimum values. However, there could be a difference in performance especially for the variance of the error on temperature due to noise. We prefer the total square error because in that case it is possible to get an expression for the computation of the temperature error variance. An analytical expression is not possible for the total absolute value, and any verification must be done using a Monte-Carlo simulation. This difficulty makes the elaboration of a design procedure for components of the technique very difficult. The total square error is given by:

$$E^2 = \sum_n \left(R_{gn} - R_{fn}\right)^2 \tag{5}$$

where R_{gn} is the ground-emitted radiance in the n^{th} band and R_{fn} is the emissivity-filtered radiance computed for band n. The algorithm structure for a given pixel is given in figure 1. It assumes that the ground-leaving radiance and the downwelling irradiance have been provided as inputs. Prior to the operation on image's pixels the algorithm initialization must be done. This step encompasses the computation of pixels' ground-leaving radiance and the downwelling irradiance for the image. Figure 1 shows the structure of the algorithm for pixel-by-pixel processing. It contains the following steps: computation of a start temperature; emissivity computation; emissivity smoothing; computation of radiance, using smoothed emissivity; computation of the total squared error on radiance; decision to stop the process and finally estimation of a new trial temperature.

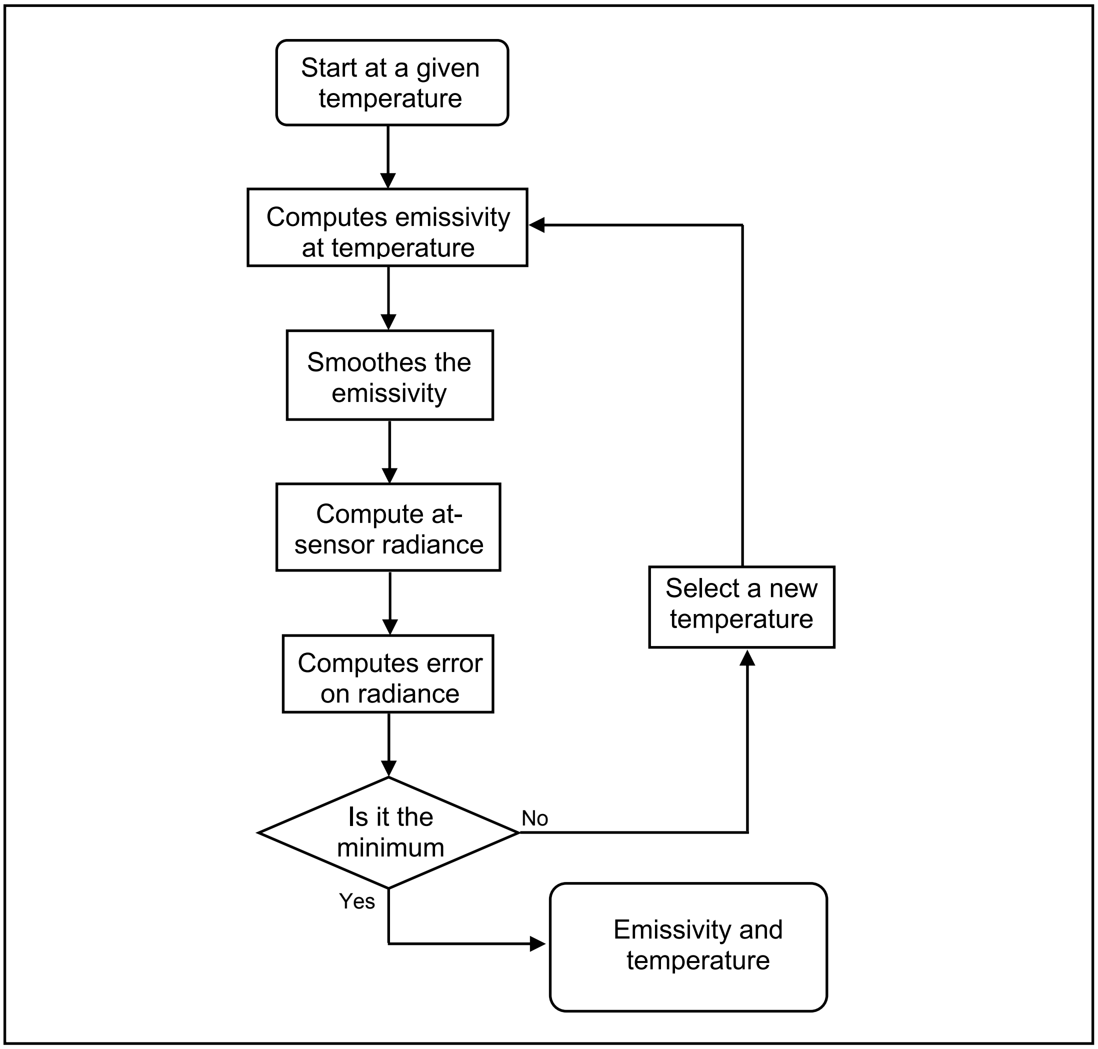

Figure 1: Structure of the proposed algorithm

3.2 Algorithm initialization

This step is not included in figure 1. The initialisation phase of the algorithm is constituted by the input of basic data, which are the image size, the atmospheric profiles or atmospheric optical parameters (transmittance, path radiance and downwelling irradiance), the sensor characteristics such as the number of bands, their centers and width and possibly there shift with lateral position also known as the smile and the sensor altitude. If the atmospheric profiles were provided, it includes the computated atmospheric optical parameters. The computation is skipped if the optical atmospheric parameters for each band are provided instead of the atmospheric profiles. The image atmospheric compensation that comprises the elimination from the data of the path radiance and of the transmittance is part of the algorithm initialisation. Another future component of the initialization is the computation of the filter's coefficients according to the weather and geographical location. This step could be added in future when a filter design technique will exist.

3.3 Pixel initialisation

Figure 1 illustrates the algorithm work for pixel processing that is the object of TES. The pixel processing needs to be started at the best possible temperature estimation. The constraint associated with the rough estimate of the temperature is that it must be within the region of stability of the algorithm and thus the estimate must be as close as possible to the true temperature of the pixel's sample. The technique uses two adjacent or nearly adjacent bands of ground-leaving radiance and their corresponding downwelling irradiance. The assumptions are: the noise can be neglected and the emissivities of the sample in the two bands are so similar that they can be assumed equal. The proximity of the two bands justifies this approximation. One very important characteristic for the selection of the two bands is that there should be a high difference in radiance due mainly to the difference in downwelling irradiance. The assumption that the emissivities are the same reduces the number of unknowns to two and therefore the problem could be solved with some small error. The two equations become:

$$\begin{aligned} \boldsymbol{R}_1 &= \varepsilon \boldsymbol{B}_1(\boldsymbol{T}) + (1-\varepsilon)\boldsymbol{L}_1 \\ \boldsymbol{R}_2 &= \varepsilon \boldsymbol{B}_2(\boldsymbol{T}) + (1-\varepsilon)\boldsymbol{L}_2 \end{aligned} \tag{7}$$

where the index of the blackbody functions indicates one band and it's nearest neighbour. Another approximation can be done that assumes the blackbody functions for the two bands are equal. The equation set becomes linear and the estimate for temperature becomes:

$$\boldsymbol{T}_{coarse} = \boldsymbol{B}_1^{-1}\left(\frac{\boldsymbol{R}_1\boldsymbol{L}_2 - \boldsymbol{R}_2\boldsymbol{L}_1}{\left(\boldsymbol{R}_1 - \boldsymbol{R}_2\right) + \left(\boldsymbol{L}_2 - \boldsymbol{L}_1\right)}\right) \tag{8}$$

3.4 Emissivity computation

The emissivity computation is the first step performed in the iteration loop on temperature, as given by equation (9).

$$\varepsilon = \frac{\boldsymbol{R}_g - \boldsymbol{L}}{\boldsymbol{B} - \boldsymbol{L}} \tag{9}$$

3.5 Emissivity filtering

Emissivity filtering is one of the critical parts of the algorithm. The filter behaviour determines to a large extent the capability of the algorithm to estimate the temperature with precision. In previous versions of the algorithm the filter was constituted around a smoothing process. The fitting of a polynomial and the computation results of a smoothed version of the emissivity were used afterwards to compute the error. This technique is reasonably good for the case of emissivities containing only small variations. If an emissivity happens to be very variable the order of the polynomial required to fit it becomes too large so the coefficients cannot be estimated accurately. The method is bounded by the use of a polynomial order lower or equal to 5.

In the analysis of that method it has been observed that the smoothing process is linear and can be described by the use of a linear filter applied to the emissivity vectors. This suggested the use of such filter for application on the emissivity. However, neither a theory for the result's evaluation or the design of such filters has been identified in the literature in this kind of application. The application of the filter on the emissivity is given by:

$$\bar{\varepsilon} = \boldsymbol{G}\varepsilon \tag{10}$$

where ε is the emissivity, G is the matrix filter, and $\bar{\varepsilon}$ is the filtered emissivity.

3.6 Radiance estimation

The radiance estimation is a simple step performed once the emissivity has been filtered. The equation is the following:

$$R_f = \bar{\varepsilon}\bar{B} + (1 - \bar{\varepsilon})L \tag{11}$$

where R_f is the radiance computed with the filtered emissivity, $\bar{B}$ is the blackbody function computed at the trial temperature and $\bar{\varepsilon}$ is the filtered emissivity.

3.7 Error estimation

The error estimation is calculated using the following expression for the total square error.

$$E^2 = \sum_n (R_{gn} - R_{fn})^2 \tag{12}$$

If the total absolute error is preferred the equation is:

$$E = \sum_n |R_{gn} - R_{fn}| \tag{13}$$

3.8 Decision

The decision to terminate the pixel processing or to modify the temperature is based on the simplex method. The algorithm is initialized with a step on temperature that is set at one degree. Initially the temperature is supposed to be a small amount under the computed minimal temperature so the initial direction of movement for the temperature is upward. Each time a temperature is updated, the error must be computed. If the error decreases, the temperature direction and step are maintained. When the error increases, even just a little bit, the temperature movement direction is reversed and the step is decreased. That procedure is followed until the temperature step reaches a minimum value. The temperature generating the minimum error value at the smaller temperature step is selected as the pixel temperature. Figure 2 shows graphically this procedure.

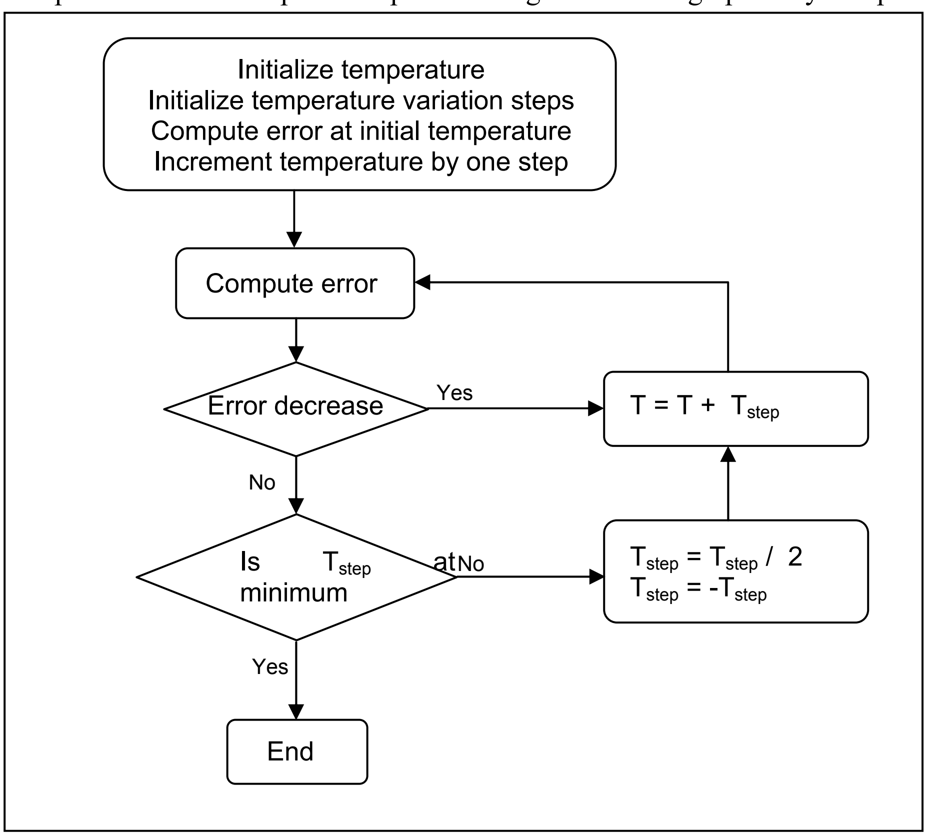

Figure 2: Description of the minimum search algorithm.

The algorithm operation has been described as a system. Improvements could probably be added in the general operation such as the variation in temperature steps or the temperature adaptation could be modified using a different procedure with the use of Newton-Raphson method or steepest descent algorithm. In any case this constitutes a rather minor modification compared to the design of adequate filters or the use of a different criterion for temperature selection.

4.0 NOISE SENSITIVITY ANALYSIS

4.1 Introduction

Sensor noise is the only impairment that will always be present in any measurement system. All other problems could be avoided or greatly reduced by modeling and processing. These other problems are related to the estimation of the required variables of the system (the downwelling irradiance, the transmittance, the path radiance and the emissivity variations). It is reasonable to think that the optical atmospheric parameters as well as the sensor's parameters will be thoroughly known for a given sensor and measurement setup so, here, we limit ourselves to the evaluation of the impacts of sensor noise on the temperature and emissivity estimation. What is required are the temperature introduced bias and the variance of the temperature estimation due to noise.

4.2 Temperature bias due to noise

We begin with the total square error as a function of temperature.

$$\boldsymbol{E}^2 = \sum_n \left(\boldsymbol{R}_{gn} - \overline{\boldsymbol{B}}\boldsymbol{G}\left(\frac{\boldsymbol{R}_g - \boldsymbol{L}}{\boldsymbol{B} - \boldsymbol{L}}\right) + \left(1 - \boldsymbol{G}\left(\frac{\boldsymbol{R}_g - \boldsymbol{L}}{\boldsymbol{B} - \boldsymbol{L}}\right)\right)\boldsymbol{L} \right)^2 \tag{14}$$

The measured radiance is given by:

$$\boldsymbol{R}_g = \varepsilon \boldsymbol{B} + (1 - \varepsilon)\boldsymbol{L} + \boldsymbol{N} \tag{15}$$

Assuming the blackbody function can be expanded in a Taylor series for the region near the temperature of interest, the total square error containing noise can be expressed by:

$$\boldsymbol{E}^2 = \sum \left(\begin{array}{l} \left(-\varepsilon_o \boldsymbol{B}_1 \boldsymbol{T}_d \boldsymbol{G}\left(\frac{1}{\boldsymbol{B}_o - \boldsymbol{L}}\right) - \boldsymbol{G}\left(\frac{\boldsymbol{N}}{\boldsymbol{B}_o - \boldsymbol{L}}\right) + \boldsymbol{B}_1 \boldsymbol{T}_d \boldsymbol{G}\left(\frac{\boldsymbol{N}}{(\boldsymbol{B}_o - \boldsymbol{L})^2}\right)\right)(\boldsymbol{B}_o - \boldsymbol{L}) + \boldsymbol{N} \\ -\left(\varepsilon_o - \varepsilon_o \boldsymbol{B}_1 \boldsymbol{T}_d \boldsymbol{G}\left(\frac{1}{\boldsymbol{B}_o - \boldsymbol{L}}\right) - \boldsymbol{G}\left(\frac{\boldsymbol{N}}{\boldsymbol{B}_o - \boldsymbol{L}}\right) + \boldsymbol{B}_1 \boldsymbol{T}_d \boldsymbol{G}\left(\frac{\boldsymbol{N}}{(\boldsymbol{B}_o - \boldsymbol{L})^2}\right)\right)\boldsymbol{B}_1 \boldsymbol{T}_d \end{array} \right)^2 \tag{16}$$

Using the fact that $\boldsymbol{B}(\boldsymbol{T}) \approx \boldsymbol{B}_o + \boldsymbol{B}_1 \boldsymbol{T}_d$

Where B_o is the blackbody function at the temperature of the target and B_1 is the first order derivative of the blackbody function estimated at the target's temperature. T_d is the deviation from that temperature that is introduced by noise and ε_o is the true emissivity of the target.

This function is quadratic on temperature and is valid in the region around the target's temperature. In this function all the variables are fixed or supposed to be known in a given case. Then to find the best estimate for the temperature one only has to minimize the function by differentiating the error function with respect to temperature and equating the derivative to zero to extract the temperature as a function of all the other variables. With a little rearrangement the derivative becomes.

$$\frac{dE^2}{dT_d} = 2\sum \left(\begin{array}{l} \left(\begin{array}{l} (B_o - L)(U - G)\left(\frac{N}{B_o - L}\right) + \\ \left((B_o - L)B_1 G\left(\frac{N}{(B_o - L)^2}\right) - \varepsilon_o B_1 (U - G)\left(\frac{1}{B_o - L}\right) + B_1 G\left(\frac{N}{B_o - L}\right)\right) T_d + \\ + \left(\varepsilon_o B_1^2 G\left(\frac{1}{B_o - L}\right) - B_1^2 G\left(\frac{N}{(B_o - L)^2}\right)\right) T_d^2 \end{array} \right) * \\ * \left(\begin{array}{l} \left((B_o - L)B_1 G\left(\frac{N}{(B_o - L)^2}\right) - \varepsilon_o B_1 (U - G)\left(\frac{1}{B_o - L}\right) + B_1 G\left(\frac{N}{B_o - L}\right)\right) + \\ + 2\left(\varepsilon_o B_1^2 G\left(\frac{1}{B_o - L}\right) - B_1^2 G\left(\frac{N}{(B_o - L)^2}\right)\right) T_d \end{array} \right) \end{array} \right) = 0 \quad (17)$$

This expression is very complicated and a lot of terms contained inside it possess a low magnitude compared to major terms. A study of each term's behaviour and magnitude near the minimum temperature is needed. The contrast between the ground and the sky radiances is the signal component possessing the highest magnitude in the above expression. Following that magnitude, are second order components such as the noise and the radiance difference due to the difference in temperature T_d. The emissivity possesses a magnitude of 1 and the temperature difference is expected to be very small if B_1T_d is considered to have a magnitude at least comparable to the noise. Neglecting the smaller terms with the use of the preceding arguments and inverting equation 17 for temperature difference leads to:

$$T_d = \frac{\sum \left(\varepsilon_o B_1 (B_o - L)^2 (U - G)\left(\frac{N}{B_o - L}\right)(U - G)\left(\frac{1}{B_o - L}\right)\right)}{\sum \left(\varepsilon_o B_1 (B_o - L)(U - G)\left(\frac{1}{B_o - L}\right)\right)^2} \quad (18)$$

This expression provides the bias due to noise in a given single case, where the noise would be known. The temperature estimate is unbiased if the noise magnitude is low enough and if the noise mean is null. To be valid expression 18 requires a high signal to ratio.

4.3 Temperature Variance due to noise

The variance of the temperature estimation can be estimated directly from these equations and gives:

$$\sigma_T^2 = \frac{\sum_i \langle b_i^2 \rangle \sum_n \left(a_n^2 M_{ni}^2 + 2a_n M_{ni} \sum_{m=n+1} a_m M_{mi} \right)}{Q^2} \quad (19)$$

Where:

$$b_i = \left(\frac{N}{B_o - L}\right)_i \text{ and then } \langle b_i^2 \rangle = \left(\frac{\langle N^2 \rangle}{(B_o - L)^2}\right)_i \quad (20)$$

$$a_n = \left[\varepsilon_o B_1 (B_o - L)^2 (U - G)\left(\frac{1}{B_o - L}\right)\right]_n \quad (21)$$

$$M = U - G \quad (22)$$

$$Q^2 = \left[\sum \left(\varepsilon_o B_1 (B_o - L)(U - G) \left(\frac{1}{B_o - L} \right) \right)^2 \right]^2 \tag{23}$$

4.4 Results comparisons of simulations and computations

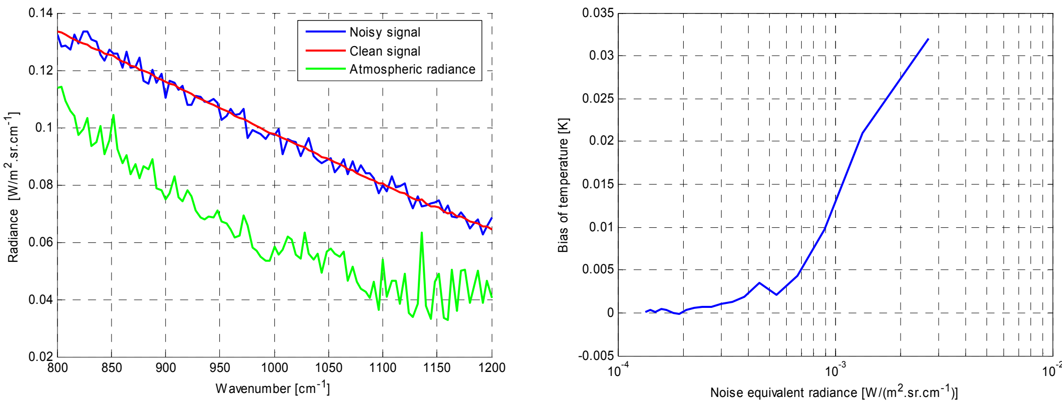

Figure 3: Example of a noisy signal in the first graph for which the red curve radiance is computed using a unitary emissivity and noise of a high magnitude is added. Second graph shows the bias on the estimated temperature for a case where the noise standard deviation is constant and indicated on the abscissa, is the same for each band and the basis signal is computed using a 0.96 constant emissivity and a temperature of 300K. The downwelling irradiance is computed using MODTRAN standard tropical atmosphere.

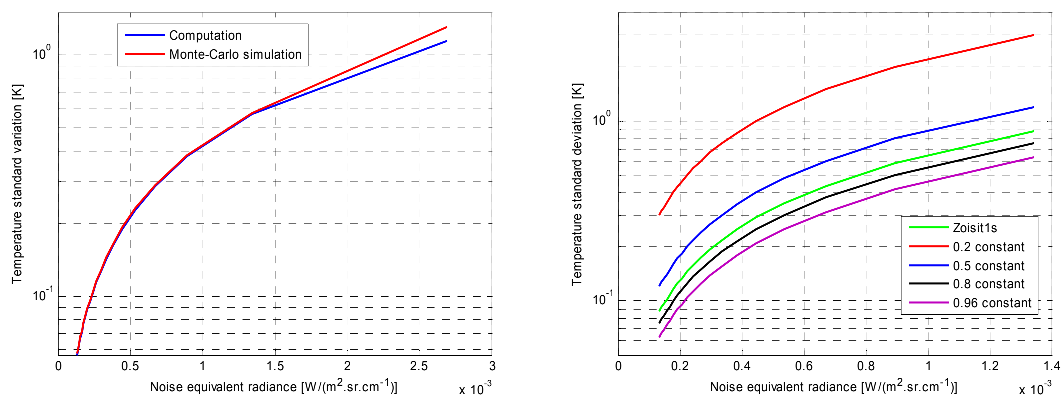

Figure 4: The left graphics shows a comparison between the standard deviation computed with equation 19 and a MODTRAN standard tropical atmosphere and a Mont-Carlo simulation in the same condition. The temperature of the sample is 300K. Right graphics shows the impact of emissivity value on the temperature standard deviation.

Figures 3 and 4 show some of the performance of the algorithm in simulations. In these simulations and estimation, there is no consideration of the effect on the estimated temperature for errors on atmospheric optical parameters. The temperature of the samples is 300K and the atmosphere is the MODTRAN standard tropical atmosphere. The contrast is therefore very low for these conditions since it is expected that for daylight condition the temperatures of surface materials should be much higher. The tropical atmosphere is also very hot and wet. It is believed according to Ingram and Muse that this represents challenging conditions for the algorithm. This is in agreement with the downwelling irradiance of the left hand graphics of figure 3 where the contrast is effectively very small. The left graph of figure 4 and the right graph of figure 3 shows that expression 19 could effectively be used and yield good results for the estimation of the temperature estimate standard deviation once the atmospheric conditions and sensor's characteristics are well known and when the signal to noise ratio is good.

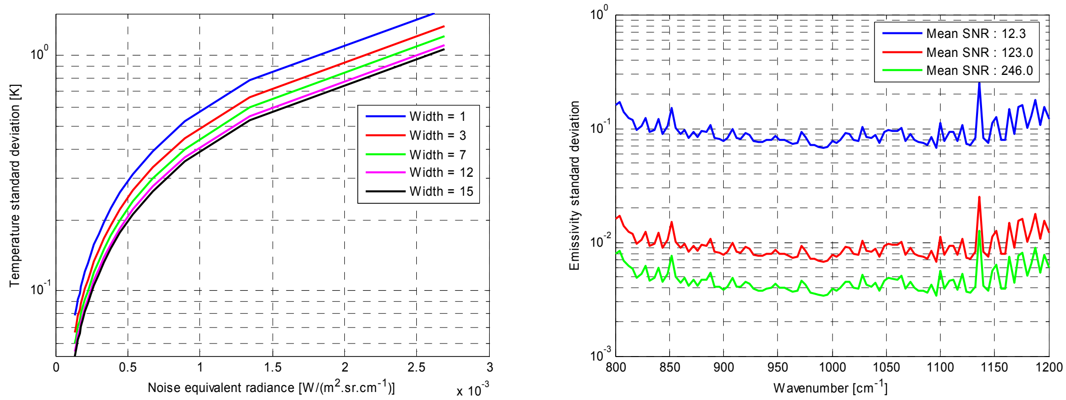

Figure 5: Left graph represents the impact of the filter's characteristics (filter width) on the estimation of the temperature. The emissivity is constant at 0.96. The right graph is the standard deviation for the emissivity given a mean signal to noise ratio for the whole sensor signal.

The width of a filter represents its capability to follow fast variations in the emissivity. The narrower it is the faster it can adapt to fast variations. The estimation of the temperature for such a fast varying emissivity will therefore be better using a narrow filter. However, the right graph of figure 4 also shows that the wider a filter is, the smaller the standard deviation will be. A compromise should therefore be made relatively to the filter that will be used in a given situation. It is interesting to note that in the formalism, there is no requirement for all the lines of a filter to be equivalent. It means that some part of the filter can be faster to adapt while other parts are slower. This complicates enormously the filter design by providing a very high level of freedom for a design procedure. One should therefore be very clever in specifying constraints.

5.0 GROUND MEASUREMENT EXAMPLE

In this section we show some results obtained through ground measurements during June of 2005. These measurements are mostly used to show that the signal model, assuming lambertian reflections, can be used in a general way. They were performed in an open area of DRDC-Valcartier, where there are no high building in the direct vicinity.

The measurement setup consists of an ABB-Bomem MR300 spectrometer mounted on a pan and tilt device. The spectrometer aims a folding mirror that reflects the radiance from a target placed on the ground. The measurements were done on a sunny day during the morning and the afternoon in two different runs. To calibrate the spectrometer three measurements are made, to obtain the gain and the offset of the instrument and of the various components. A hot blackbody source is first measured, then the downwelling irradiance is measured with an infragold plate and an ambient temperature blackbody source is used. The downwelling irradiance measurement is used to compensate for the small reflections generated by the blackbodies, which possess an emissivity near 98.5%.

Three measurements examples done during the morning and the afternoon are shown at figure 6 to 8. The first target is a sandblasted aluminium panel used in airborne trials for calibrating sensors. The second target is a plain plywood panel representing typical construction material and the third is a roofing material panel.

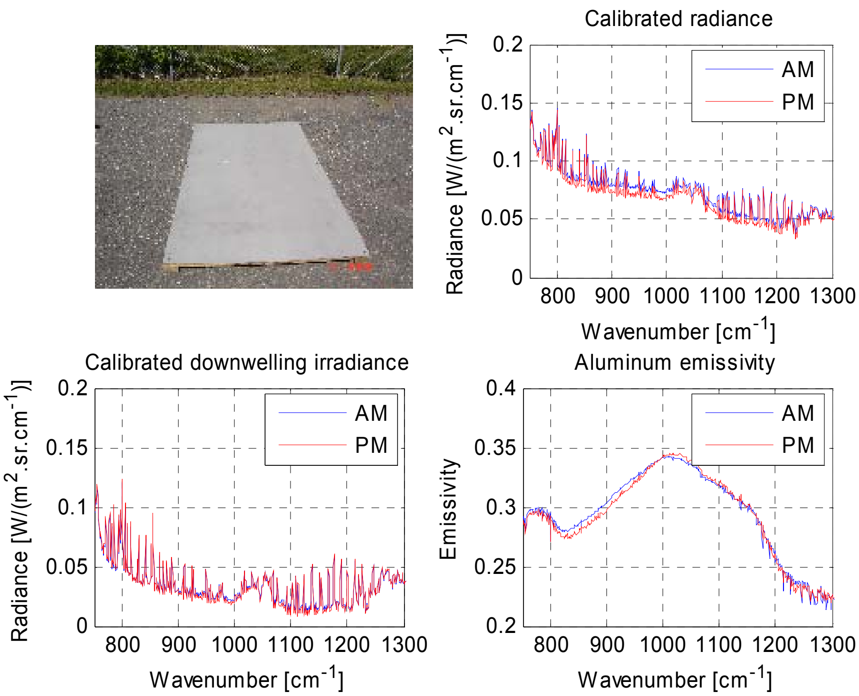

Figure 6: Aluminium panel: Panel photograph, ground-leaving radiance, downwelling irradiance and emissivity. Estimated temperature: AM 65°C, PM 59°C

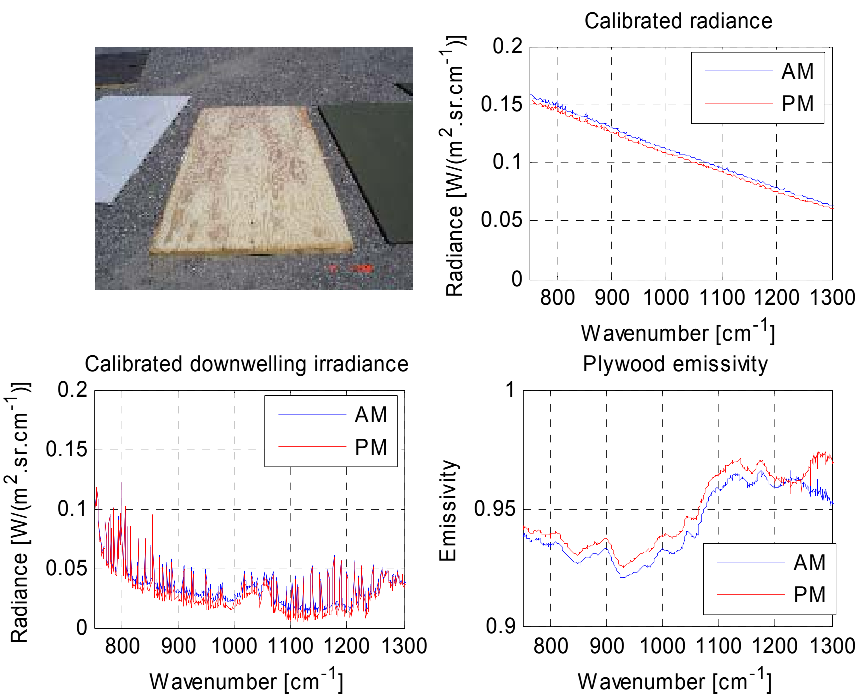

Figure 7: Plywood Panel: Photograph, ground-leaving radiance, downwelling irradiance and emissivity. Estimated temperature: AM 38.1°C PM 35.7°C

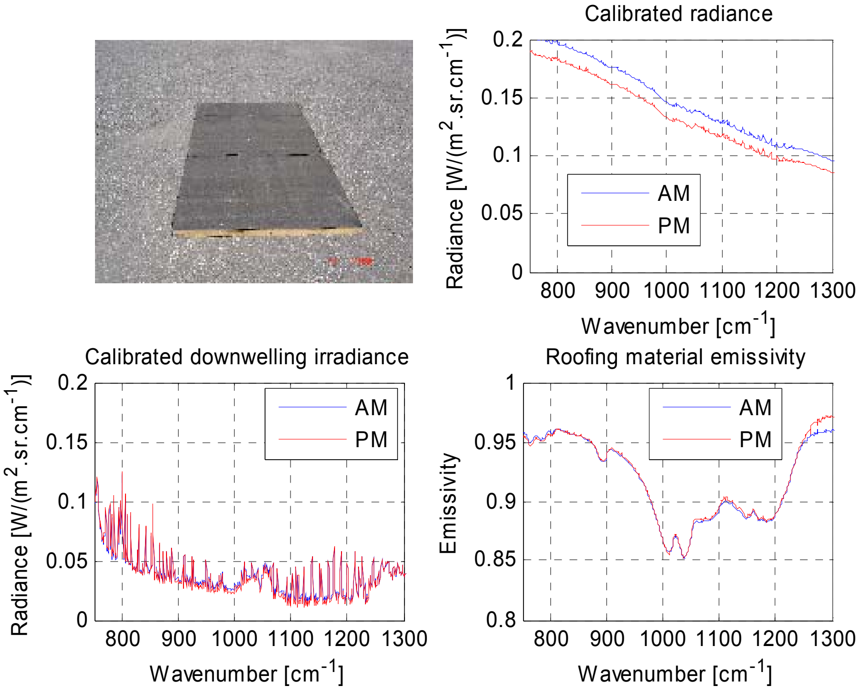

Figure 8: Roofing material: Photograph, ground-leaving radiance, downwelling irradiance and emissivity. Estimated temperature: AM 61.5°C, PM 54.5°C

The temperature estimation given in the figure caption is the temperature at which the emissivity has been computed for each samples. Temperature measurements for validation are notoriously difficult to obtain, using any kind of technique. For instance a radiometer would not provide accurate measurement for a sample such as the roofing material since the emissivity is not constant. A thermocouple placed at the surface may find a different temperature to other parts of the surface since conductivity and cooling by convection due to wind may be different. A measurement done underneath the material could also show a large difference with the surface because of the time lag due to the thickness of the material. The contact between the material and the substrate could also interfere with the measurement. These various problems complicate the task of validating the algorithms using independent measurements. The correspondence of the emissivity for each measurement is clearly seen from the emissivity figures and this fact could also be used for validating the algorithms. In this process, however, the spectrometer calibration process will have to be evaluated since there could still be error of approximately 0.5K with the calibration technique we are using. We also conclude that the surfaces, especially the aluminium panel could be assumed to be lambertian, or at least has reflection characteristics similar to these of the infragold plate used to measure the downwelling irradiance.

6.0 CONCLUSION

An algorithm for temperature and emissivity separation is proposed in this paper. It is based on the iteration on temperature principle where the temperature selection criterion is the minimum total square error between the ground-leaving radiance and a filtered emissivity counterpart of the same radiance. The computation at a given temperature involves the estimation of a trial emissivity that is filtered and re-used in the computation to determine a different radiance. The total square error is the sum of the square of the difference between the measured radiance for each sensor bands. The main components of the technique are the filters and the use of the total square error. The operational basis is that when the trial temperature will be very near the sample temperature the estimated emissivity will be smooth enough that the filtering will not modify it appreciably and therefore the total square error will be minimal at that temperature.

The system is impeded by sensor noise. We obtained mathematically an expression for the estimation of the impacts of noise in terms of the standard deviation of the temperature estimate. The expression showed a very good correspondence with Monte-Carlo simulation using the technique in the same conditions as for the computations. Experimental validation of the technique involves the characterisation of a sensor with respect to noise and the acquisition of a large number of independent measurements and the comparison with the standard deviation estimation.

The mathematical model representing the technique's operations is important, because it enables the evaluation of the effect of the main component of the method, which is the filter, with respect to different conditions. The weather, the ground temperatures and the samples' emissivities are examples of these conditions that affect the quality of the results. It is also important because it could lead to an approach for filter design adapted to maximize the precision given a particular condition of operation. Finally, it enables the assessment of the result's quality once a computation has been made on a given image. This particular aspect is of interest for people working in other field of hyperspectral image processing, because it can conditions the operations of detection algorithms and the subsequent use of imagery.

A good TES technique is also required to lay the ground for an autonomous atmospheric compensation technique, which is the future for high altitude thermal hyperspectral imagery. In this scenario, one possible scheme is the use of iteration for the atmospheric profiles leading to credible emissivity and temperature estimation related to a given pixel's spectrum.

[1] Borel, C.C, "Surface emissivity and temperature retrieval for a hyperspectral sensor", Geoscience and Remote Sensing Symposium Proceedings, 1998. IGARSS '98. 1998 IEEE, International , Volume: 1 , 6-10 July 1998, pp. 546 -549 vol.1

[2] Ingram, P.M., Muse, A.H, "Sensitivity of iterative spectrally smooth temperature/emissivity separation to algorithmic assumptions and measurement noise", Geoscience and Remote Sensing, IEEE Transactions on , Volume: 39 Issue: 10 , Oct. 2001, pp. 2158-2167